IEEE Access
Multidisciplinary | Rapid Review | Open Access Journal

Received October 11, 2019, accepted October 22, 2019, date of publication October 29, 2019, date of current version November 7, 2019.

Digital Object Identifier 10.1109/ACCESS.2019.2950016

Spherical Harmonic Atomic Norm and Its Application to DOA Estimation

JIE PAN
School of Information Engineering, Yangzhou University, Yangzhou 225009, China
e-mail: panjie@yzu.edu.cn

This work was supported in part by the National Natural Science Foundation of China under Grant 61601402, and in part by the Natural Science Foundation of Jiangsu Province under Grant BK20160477.

ABSTRACT Signal processing in the spherical harmonic (SH) domain has the advantages of analyzing a signal on the sphere with equal resolution in the whole space and of decomposite the frequency- and location-dependent components of the signal. Therefore, it finds recent applications in signal recovery and localization. In this paper, we consider the gridless sparse signal recovery problem in the SH domain with atomic norm minimization (ANM). Due to the absence of Vandermonde structure for spherical harmonics, the Vandermonde decomposition theorem, which is the mathematic foundation of conventional ANM approaches, is not applicable in the SH domain. To address this issue, a low-dimensional semidefinite programming (SDP) method to implement the spherical harmonic atomic norm minimization (SH-ANM) approach is proposed. This method does not rely on the Vandermonde decomposition and can recover the atomic decomposition in the SH domain directly. As an application, we develop the direction-of-arrival estimation approach based on the proposed SH-ANM method, and computer simulations demonstrate that its performance is superior to the state-of-the-art counterparts. Furthermore, we validate the results in real-life acoustics scenes for multiple speakers localization using measured data in LACATA challenge.

INDEX TERMS Spherical harmonic domain, atomic norm, gridless sparse signal recovery, semidefinite programming, direction-of-arrive estimation.

I. INTRODUCTION

Sherical harmonics (SH) are a set of orthogonal polynomials as the complete basis on the sphere which can be used for approximation of the spherical manifolds. It has been studied extensively to process the signals defined on the spherical manifolds encountered in practice, such as astrophysics, medical imaging, and audio processing, among others [1]–[3]. The signals on the spherical manifolds can be orthogonally projected onto the vector of spherical harmonics, which is known as spherical harmonic domain. Various signal processing approaches have been extended to the SH domain for signal recovery, direction-of-arrival (DOA) estimation, etc.

In last decades, several classical DOA estimation methods and their applications have been proposed in literatures, such as MUSIC [4], ESPRIT [5], propagator method [6], maximum likelihood [7] and tensor approaches [8], etc. Some conventional DOA estimation methods have been proposed for SH domain in [9]–[11].

Inspired by the sparse representation technique [12], [13], sparse signal processing in the SH domain has been drawn attention to in recent years. In [14], [15], sparse recovery in the SH domain for random sampling has been studied. In [16], the ℓ_1-SVD (singular value decomposition, SVD) method in the SH domain has been proposed for combating room reverberations. In [17], [18], the sparse Bayesian learning DOA estimation methods were exploited to the SH domain. The sparse Bayesian learning based methods may provide better performance than ℓ_1 norm based ones [13], and they are with slow convergence rate, however [28]. Furthermore, the aforementioned sparsity-based approaches may be degraded by the grid mismatch problem. To deal with the problem, some efforts have been made to alleviate the grid modeling error to some extent [19].

Recently, a unified framework has been proposed for sparse representation on the finite/infinite dimensional dictionary in [20]. It results in a gridless sparse recovery method

The associate editor coordinating the review of this manuscript and approving it for publication was Liangtian Wan.

by solving the optimization problem on the convex hull of an atomic set, which is known as the atomic norm minimization (ANM). Specially, for the atoms defined on the set of complex exponentials, Candès and Fernandez-Granda show that a bandlimited signal can be recovered with given number of low rate samples if the frequency separation condition holds [21]. Based on the theory, the ANM approach has been extended to multidimensional frequency models [22]–[24], prior kenowledge [25], multiple measurement vectors (MMV) [26] and covariance matrix cases [27]–[29] for gridless signal recovery and DOA estimation. However, these conventional ANM methods depend upon the Vandermonde structure of the array manifolds, and hence they are limited to linear or rectangular arrays.

To apply the ANM approach to SH domain [30], one straightforward idea is to solve the conventional ANM problem, where the atomic elements are Vandermonde vectors, with the extra weighting constraints [31], [33], [34]. This approach results in an potentially higher dimensional semidefinite programming (SDP) problem than the dimension of samples, which would be quite computational demanding.

As the extensive real-time applications for gridless sparse representation methods on the spherical manifolds, e.g. DOA estimation, it motivates us to develop the low dimensional spherical harmonic ANM approach, that is not yet reported in the literature.

In this paper, we study the gridless sparse signal recovery problem on the spherical manifolds, by means of atomic norm minimization, with its application to DOA estimation of spherical arrays. We first define the spherical harmonic atomic norm based on covariance matrix in SH domain. Due to the fact that spherical harmonics are not Vandermonde, the major challenge of extending ANM approach to SH domain is to formulate convex optimization problem in absence of Vandermonde decomposition theorem. To deal with this issue, we propose a low-dimensional SDP formulation of spherical harmonic atomic norm minimization (SH-ANM) problem, which retrieve the atomic decomposition in SH domain directly without the foundation of Vandermonde decomposition theorem. Then, we present the SH-ANM based approach for DOA estimation of spherical arrays and show the performance improvement beyond some existed methods, especially in low signal-noise ratio(SNR) and adjacent sources scenarios. Finally, we demonstrate efficacy of our method with the experimental data taken from the IEEE audio and acoustic signal processing (AASP) challenge on acoustic source localization and tracking(LOCATA) [35] in the context of speakers localization.

The paper is organized as follows. Section II introduce the SH domain wavefield model briefly and section III present the spherical harmonic atomic norm concept. The SDP formulation of SH-ANM problem and SH-ANM based signal denoising method is proposed in section IV. Consequently, SH-ANM approach is applied to DOA estimation scenario in Section V. Then the simulations and the experiments are shown in Section VI and VII. Section VIII concludes the paper.

Notations: $(\bullet)^{\mathrm{T}}$ denotes the transpose, $vec(\bullet)$ represents the vectorization operator. $(\bullet)^*$ and $(\bullet)^{\mathrm{H}}$ means complex conjugate and conjugate transpose operation. $\mathrm{Re}(\bullet)$ is the real part operator. The diagonal matrix is represented as $\mathrm{diag}(\mathbf{x})$. $\mathrm{Tr}(\bullet)$ is the trace. $\|\bullet\|_2$, $\|\bullet\|_F$ are the Euclidean and Frobenius norm respectively. $\otimes$ denotes the Kronecker product, for a matrix $\mathbf{M}$, $\mathbf{M} \geq 0$ denotes nonnegative definite. $\mathbf{I}$ denotes the identity matrix and $\delta_{k,l}$ is the Kronecker delta. $E\{\bullet\}$ is understood as the expectation.

II. SIGNAL MODEL

Consider a spherical array of I sensors, the ith element is at $\mathbf{u}_i = (R, \Phi_i)$ where $\Phi_i = (\theta_i, \varphi_i)$ and R, θ, φ are the radius, elevation and azimuth. There are K far-field sources located at $\Psi_k = (\theta_k, \varphi_k) \in \Xi$ with $\Xi = \{(\theta, \varphi) | \theta \in (0, \pi], \varphi \in (-\pi, \pi]\}$. The received signals of the spherical array $\mathbf{X}(t)$ is

$$\mathbf{X}(t) = \mathbf{A}(\vec{\Psi})\mathbf{s}(t) + \mathbf{n}(t) \tag{1}$$

where $\mathbf{s}(t)$ and $\mathbf{n}(t)$ are the source and additional noise component, respectively. The array manifold is $\mathbf{A}(\vec{\Psi}) = [\mathbf{a}(\Psi_1), \ldots, \mathbf{a}(\Psi_K)] \in \mathbb{C}^{I \times K}$.

Let $Y_n^m(\theta, \varphi)$ is the spherical harmonic of order n and degree m,

$$Y_n^m(\theta, \varphi) = \sqrt{\frac{(2n+1)(n-m)!}{4\pi(n+m)!}} P_n^m(\cos\theta) e^{im\varphi} \quad \forall 0 \leq n \leq N,\ 0 \leq m \leq n \tag{2}$$

with the associated Legendre polynomial $P_n^m(\cos\theta)$, the ith element of $\mathbf{a}(\Psi_k)$ can be represented as spherical harmonic series expansion by ignoring the high order $b_n(\kappa R)$ when $n > \kappa R$ [3]

$$a_i(\Psi_k) = \sum_{n=0}^{N} \sum_{m=-n}^{n} b_n(\kappa R)[Y_n^m(\Psi_k)]^* Y_n^m(\Phi_i) \tag{3}$$

where N is the maximum spherical harmonics order, $\kappa = \lambda/2\pi$ and λ is the wavelength. The frequency dependent component $b_n(\kappa R)$ is modeled as [3]

$$b_n(\kappa R) = \begin{cases} 4\pi i^n J_n(\kappa R) & \text{open sphere} \\ 4\pi i^n (J_n(\kappa R) - \dfrac{J'_n(\kappa R)}{u'_n(\kappa R)} u_n(\kappa R)) & \text{rigid sphere.} \end{cases} \tag{4}$$

where u_n and J_n are spherical Hankel function of second kind and spherical Bessel function of first kind, respectively. The derivatives of J_n and u_n are denoted by J'_n and u'_n.

Then, we have the matrix form of the spherical array model that

$$\mathbf{A}(\vec{\Psi}) = \mathbf{Y}(\vec{\Phi})\mathbf{B}\mathbf{Y}^{\mathrm{H}}(\vec{\Psi}) \tag{5}$$

where the ith raw vector of $\mathbf{Y}(\vec{\Phi}) \in \mathbb{C}^{I \times (N+1)^2}$ and the kth raw vector of $\mathbf{Y}(\vec{\Psi}) \in \mathbb{C}^{K \times (N+1)^2}$ is

$$\mathbf{y}(\Phi_i) = [Y_0^0(\Phi_i), Y_1^{-1}(\Phi_i), Y_1^0(\Phi_i), \ldots, Y_N^N(\Phi_i)],$$

$$\mathbf{y}(\Psi_k) = [Y_0^0(\Psi_k), Y_1^{-1}(\Psi_i), Y_1^0(\Psi_k), \ldots, Y_N^N(\Psi_k)] \quad (6)$$

and $\mathbf{B} \in \mathbb{C}^{(N+1)^2 \times (N+1)^2}$ is given by

$$\mathbf{B} = \mathrm{diag}\left(b_0(\kappa R), \ldots, b_N(\kappa R)\right). \quad (7)$$

Accordingly, we apply SH domain transformation as

$$\begin{aligned}\mathbf{P}(t) &= \mathbf{Y}^{\mathrm{H}}(\vec{\Phi})\Gamma\mathbf{X}(t) \\ &= \mathbf{B}\mathbf{Y}^{\mathrm{H}}(\vec{\Psi})\mathbf{s}(t) + \mathbf{v}(t)\end{aligned} \quad (8)$$

where $\Gamma = \mathrm{diag}(\alpha_1, \alpha_2, \ldots, \alpha_I)$ is satisfying [3], [50]

$$\mathbf{Y}^{\mathrm{H}}(\vec{\Phi})\Gamma\mathbf{Y}(\vec{\Phi}) = \mathbf{I}. \quad (9)$$

and $\mathbf{v}(t)$ is the transformed additional noise. Therefore, the covariance matrix in SH domain is given by

$$\begin{aligned}\mathbf{R} &= E\left\{\mathbf{P}(t)\mathbf{P}^{\mathrm{H}}(t)\right\} \\ &= \mathbf{B}\mathbf{Y}^{\mathrm{H}}(\vec{\Psi})\mathbf{R}_s\mathbf{Y}(\vec{\Psi})\mathbf{B}^{\mathrm{H}} + \mathbf{V}\end{aligned} \quad (10)$$

with $\mathbf{V} = E\left\{\mathbf{v}(t)\mathbf{v}^{\mathrm{H}}(t)\right\}$ and $\mathbf{R}_s = E\left\{\mathbf{s}(t)\mathbf{s}^{\mathrm{H}}(t)\right\}$. It is remarked that if $E\left\{\mathbf{n}(t)\mathbf{n}^{\mathrm{H}}(t)\right\} = \sigma^2\mathbf{I}$ (σ^2 is the power of noise) and the location of spherical array elements $\vec{\Phi}$ obeys spherical t-design distribution in [3]($\Gamma = \mathbf{I}$), then $\mathbf{V} = \sigma^2\mathbf{I}$.

Denote the ith column of matrix $\mathbf{R}$ in (10) as $\mathbf{r}_i$, it can be regarded as a single measurement of the array. Thus, let $\mathbf{H} = \mathbf{R}_s\mathbf{Y}(\vec{\Psi})\mathbf{B}^{\mathrm{H}}$, we can remodel $\mathbf{r}_i$ as

$$\begin{aligned}\mathbf{r}_i &= E\left\{\mathbf{P}(t)\boldsymbol{p}_i^*(t)\right\} \\ &= \mathbf{B}\mathbf{Y}^{\mathrm{H}}(\vec{\Psi})\mathbf{h}_i + \mathbf{v}_i\end{aligned} \quad (11)$$

where $\boldsymbol{p}_i(t)$ is the ith row of $\mathbf{P}(t)$, $\mathbf{h}_i$ and $\mathbf{v}_i$ are the ith column of $\mathbf{H}$ and $\mathbf{V}$, respectively. By (10) and (11), the matrix form of covariance matrix in SH domain in (10) is [36]

$$\begin{aligned}\mathbf{R} &= \mathbf{B}\mathbf{Y}^{\mathrm{H}}(\vec{\Psi})\mathbf{H} + \mathbf{V} \\ &= \sum_{k=1}^{K} c_k\mathbf{B}\mathbf{Y}^{\mathrm{H}}(\Psi_k)\boldsymbol{\rho}_k + \mathbf{V}\end{aligned} \quad (12)$$

where c_k is the Euclidean norm of kth raw vector of $\mathbf{H}$ and $\boldsymbol{\rho}_k$ denotes the normalized kth raw vector of $\mathbf{H}$, i.e. $\|\boldsymbol{\rho}_k\|_2 = 1$.

Observe that the covariance matrix $\mathbf{R}$ in (12) reveals a Multiple Measurement Vectors (MMV) formulation, by which we shall propose a novel compact formulation of the atomic norm for the covariance matrix in next section.

III. SPHERICAL HARMONIC ATOMIC NORM

Following the scheme proposed by Chandrasekaran *et al.* [20], we can define an atomic set where the elements are the basis of the representation to the signals analyzed. For the signals in SH domain, the atomic set $\mathcal{A}$ depends on the atoms of the spherical harmonic vectors $\mathbf{Y}(\Psi)$ and the signals can be described as a sum of distinct atoms

$$\mathbf{x} = \sum_{k=1}^{K} c_{\Psi_k}\mathbf{Y}(\Psi_k), \qquad \mathbf{Y}(\Psi_k) \in \mathcal{A}. \quad (13)$$

The decomposition in (13) is known as an atomic decomposition.

Finding the sparsest atomic decomposition of $\mathbf{x}$ results in the l_0 spherical harmonic atomic norm as

$$\|\mathbf{x}\|_{\mathcal{A},0} = \inf\left\{K | \mathbf{x} = \sum_{k=1}^{K} c_{\Psi_k}\mathbf{Y}(\Psi_k), \mathbf{Y}(\Psi_k) \in \mathcal{A}\right\}. \quad (14)$$

To recover the signal within a convex optimization framework, [20] suggests a convex heuristic of the l_0 atomic norm, which is denoted by

$$\|\mathbf{x}\|_{\mathcal{A}} = \inf\left\{t > 0 : x \in t\ conv(\mathcal{A})\right\}, \quad (15)$$

where $conv(\mathcal{A})$ is the convex hull of $\mathcal{A}$. Thus, we have

$$\|\mathbf{x}\|_{\mathcal{A}} = \inf\left\{\sum_{k=1}^{K} c_{\Psi_k} | \mathbf{x} = \sum_{k=1}^{K} c_{\Psi_k}\mathbf{Y}(\Psi_k), \mathbf{Y}(\Psi_k) \in \mathcal{A}\right\}, \quad (16)$$

which is named spherical harmonic atomic norm and the corresponding dual norm $\|\bullet\|_{\mathcal{A}}^*$ is [37]

$$\|\mathbf{x}\|_{\mathcal{A}}^* = \sup_{\|\mathbf{q}\|_{\mathcal{A}} \le 1} \mathrm{Re}\left\{\mathrm{Tr}\left[\mathbf{x}^{\mathrm{H}}\mathbf{q}\right]\right\} \quad (17)$$

For the application of DOA estimation, various kinds of atomic norms are developed for covariance matrix in [27]–[29]. Here, we propose a new atomic norm of the covariance for DOA estimation of the spherical arrays.

Observe the MMV model of the noiseless covariance matrix in (12) that $\mathbf{R} = \sum_{k=1}^{K} c_k\mathbf{B}\mathbf{Y}^{\mathrm{H}}(\Psi_k)\boldsymbol{\rho}_k$, we define the spherical harmonic atomic set as

$$\mathcal{A} := \left\{\mathbf{B}\mathbf{Y}^{\mathrm{H}}(\Psi)\boldsymbol{\rho} \,\middle|\, \Psi \in \Xi, \|\boldsymbol{\rho}\|_2 = 1\right\}. \quad (18)$$

Thus, we define the spherical harmonic atomic l_0 norm of the covariance matrix $\mathbf{R}$ as

$$\|\mathbf{R}\|_{\mathcal{A},0} = \inf\left\{K \,|\, \mathbf{R} = \sum_{k=1}^{K} c_k\mathbf{B}\mathbf{Y}^{\mathrm{H}}(\Psi_k)\boldsymbol{\rho}_k . c_k \ge 0\right\}, \quad (19)$$

and the spherical harmonic atomic norm of $\mathbf{R}$ as

$$\|\mathbf{R}\|_{\mathcal{A}} = \inf\left\{\sum_{k=1}^{K} c_k \,\middle|\, \mathbf{R} = \sum_{k=1}^{K} c_k\mathbf{B}\mathbf{Y}^{\mathrm{H}}(\Psi_k)\boldsymbol{\rho}_k, c_k \ge 0\right\}. \quad (20)$$

Regarding the spherical harmonic atomic norm defined above, we have the following remarks:

Remark 1: Our spherical harmonic atomic norm of covariance matrix defined in (20) can be regarded as the atomic norm for MMV model from the perspective of the representation in (12), and also can be interpreted as an extension of the atomic norm for single measurement vector (SMV) by averaging over the snapshots. That is similar to the idea presented in [38], but our atomic norm is without the limitation of the non-zero mean assumption over the original sources since the covariance matrix is positive semidefinite.

Remark 2: Unlike dimensional reduction technique presented in [39] for ANM problem in MMV case, the proposed spherical harmonic atomic norm does not require additional computations, such as QR decomposition or square rooting of the covariance matrix.

Remark 3: The proposed spherical harmonic atomic norm can be referred to as a kind of nuclear norm as defined in [28] for the uncorrelated signals, but it does not depend on the uncorrelated signals assumption which is different from [28]. It implies that the proposed method has the robustness to the correlated or even coherent signals, which can be found in various applications of radar, sonar and wireless communication [40].

IV. SEMIDEFINITE PROGRAMMING TO SOLVE SPHERICAL HARMONIC ATOMIC NORM MINIMIZATION

The conventional ANM methods for linear spectrum relies on the Vandermonde decomposition theorem to construct the equivalent SDP implementation. Unfortunately, this approach cannot be extended to SH-ANM problem in (20) directly, due to the fundamental difficulty that vectors of spherical harmonics are not with Vandermonde structure. To deal with this issue, we develop an SDP formulation for the SH-ANM problem in this section.

A. SDP IMPLEMENTATION OF SH-ANM

Note that $P_n^m(\cos\theta)$ is a order n trigonometric polynomial that $P_n^m(\cos\theta) = \sum_{l=-n}^{n} \beta_{n,m,l} e^{il\theta}$ with unique coefficients $\{\beta_{n,k,l}\}$, the spherical harmonic in (2) can be expressed by 2-D Fourier series as [34]

$$Y_n^m(\theta,\varphi) = \sum_{l=-n}^{n} A_{n.m}\beta_{n,m,l} e^{il\theta} e^{im\varphi} \tag{21}$$

where $A_{n.m} = \sqrt{\frac{(2n+1)(n-m)!}{4\pi(n+m)!}}$. By (21), we can rewrite (8) as

$$\mathbf{P}(t) = \mathbf{B}\mathbf{G}\mathbf{D}(\vec{\Psi})\mathbf{s}(t) + \mathbf{v}(t) \tag{22}$$

where $\mathbf{D}(\vec{\Psi}) = [\mathbf{f}(\Psi_1), \ldots, \mathbf{f}(\Psi_K)]$ with

$$\begin{aligned}
\mathbf{f}(\Psi_k) &= \mathbf{f}_\theta(\theta_k) \otimes \mathbf{f}_\varphi(\varphi_k),\\
\mathbf{f}_\theta(\theta_k) &= \left[e^{-iN\theta_k}, \ldots, 1, \ldots, e^{iN\theta_k}\right]^{\mathrm{T}},\\
\mathbf{f}_\varphi(\varphi_k) &= \left[e^{-iN\varphi_k}, \ldots, 1, \ldots, e^{iN\varphi_k}\right]^{\mathrm{T}},
\end{aligned} \tag{23}$$

and $\mathbf{G}$ is a constant matrix constructed by $A_{n.m}$, $\beta_{n,m,l}$. Therefore, substituting (22) into (12), we have

$$\begin{aligned}
\mathbf{R} &= E\left\{\mathbf{P}(t)\mathbf{P}^{\mathrm{H}}(t)\right\}\\
&= \tilde{\mathbf{G}}\mathbf{D}(\vec{\Psi})\mathbf{R}_s\mathbf{D}^{\mathrm{H}}(\vec{\Psi})\tilde{\mathbf{G}}^{\mathrm{H}} + \mathbf{V}
\end{aligned} \tag{24}$$

with $\tilde{\mathbf{G}} = \mathbf{B}\mathbf{G}$.

By utilizing the relationship revealed in (24) about the SH domain steering vector and Vandermonde matrix, we start with the noise-free case where $\mathbf{V} = 0$ and develop the following low dimensional SDP implementation for SH-ANM approach.

Theorem 1: Given the location of sources $\vec{\Psi}$, let minimizing the objective value of the following optimization problem yield the norm $\|\mathbf{R}\|_{\mathrm{T}}$, i.e.

$$\|\mathbf{R}\|_{\mathrm{T}} = \min_{\mathbf{Q},\mathbf{M}} \frac{1}{2\zeta^2}\mathrm{Tr}(\tilde{\mathbf{G}}S(\mathbf{Q})\tilde{\mathbf{G}}^{\mathrm{H}}) + \frac{1}{2}\mathrm{Tr}(\mathbf{M})$$

$$\text{s.t.} \quad \begin{bmatrix} \tilde{\mathbf{G}}S(\mathbf{Q})\tilde{\mathbf{G}}^{\mathrm{H}} & \mathbf{R} \\ \mathbf{R}^{\mathrm{H}} & \mathbf{M} \end{bmatrix} \geq 0, \tag{25}$$

if the maximum spherical harmonics order N is sufficiently high and strong duality holds, we have $\|\mathbf{R}\|_{\mathrm{T}} = \|\mathbf{R}\|_{\mathcal{A}}$, where $\|\mathbf{R}\|_{\mathcal{A}}$ is the spherical harmonic atomic norm defined in (20) with $\mathbf{R} \in \mathbb{C}^{(N+1)^2\times(N+1)^2}$.

$$\zeta = \left\|\tilde{\mathbf{G}}\right\|_F = \sqrt{\sum_{l=0}^{N} \frac{(4l+1)}{4\pi}} \|\mathbf{B}\|_F, \tag{26}$$

and $S(\mathbf{Q})$ is a Hermitian matrix consisted of $\mathbf{Q}$ as [22]

$$S(\mathbf{Q}) = \begin{bmatrix} \mathbf{Q}_0 & \mathbf{Q}_{-1} & \cdots & \mathbf{Q}_{-2N} \\ \mathbf{Q}_1 & \mathbf{Q}_0 & \cdots & \mathbf{Q}_{-2N+1} \\ \vdots & \vdots & \ddots & \vdots \\ \mathbf{Q}_{2N} & \mathbf{Q}_{2N-1} & \cdots & \mathbf{Q}_0 \end{bmatrix} \tag{27}$$

with $\mathbf{Q}_l$ is a Toeplitz matrix defined by lth row of $\mathbf{Q}$ as

$$\mathbf{Q}_l = \begin{bmatrix} q_{l,0} & q_{l,-1} & \cdots & q_{l,-2N} \\ q_{l,1} & q_{l,0} & \cdots & q_{l,-(2N-1)} \\ \vdots & \vdots & \ddots & \vdots \\ q_{l,2N} & q_{l,2N-1} & \cdots & q_{l,0} \end{bmatrix}. \tag{28}$$

We prove this theorem in Section IV-B based on the sum-of-squares relaxation of polynomial and the equivalence between the prime and dual problem followed by strong duality.

B. PROOF OF THEOREM 1

Easy to show that $\|\mathbf{R}\|_{\mathrm{T}} \leq \|\mathbf{R}\|_{\mathcal{A}}$ (See [37]), However, there is no guarantee to ensure the positive semidefinite property of $S(\mathbf{Q})$, and thus we are not sure there exists a Vandermonde decomposition for the two folds block Toeplitz matrix $S(\mathbf{Q})$. Consequently, the conventional proof procedure for $\|\mathbf{R}\|_{\mathrm{T}} \geq \|\mathbf{R}\|_{\mathcal{A}}$ proposed in [23], [26], [37] is not applicable in our case.

To investigate the relationship between SDP implementation in (25) and the original spherical harmonic atomic norm in (20), we alternate the route to the dual problem.

Following the definition of the dual norm in (17), the dual spherical harmonic atomic norm of the covariance matrix $\mathbf{R}$ is repesented as

$$\begin{aligned}
\|\mathbf{R}\|_{\mathcal{A}}^* &= \sup_{\|\Omega\|_{\mathcal{A}}\leq 1} \mathrm{Re}\left\{\mathrm{Tr}\left[\mathbf{R}^{\mathrm{H}}\Omega\right]\right\}\\
&= \sup_{\Psi\in\Xi, \|\boldsymbol{\rho}\|_2=1} \mathrm{Re}\left\{\mathrm{Tr}\left[\mathbf{R}^{\mathrm{H}}\mathbf{B}\mathbf{Y}^{\mathrm{H}}(\Psi)\boldsymbol{\rho}\right]\right\}\\
&= \sup_{\Psi\in\Xi, \|\boldsymbol{\rho}\|_2=1} \left|\mathrm{Tr}\left[\boldsymbol{\rho}\mathbf{R}^{\mathrm{H}}\mathbf{B}\mathbf{Y}^{\mathrm{H}}(\Psi)\right]\right|\\
&= \sup_{\Psi\in\Xi} \left\|\mathbf{R}^{\mathrm{H}}\mathbf{B}\mathbf{Y}^{\mathrm{H}}(\Psi)\right\|_2.
\end{aligned} \tag{29}$$

By the Largrangian analysis, we have the dual problem of (20)

$$\max_{\Omega} \mathrm{Re}\left\{\mathrm{Tr}\left[\mathbf{R}^{\mathrm{H}}\Omega\right]\right\}$$

$$\text{s.t.} \quad \|\Omega\|_{\mathcal{A}}^* \le 1, \tag{30}$$

and propose the following SDP implementation of the dual SH-ANM problem based on the sum-of-squares relaxation of polynomials [24].

Theorem 2: Given the location of sources $\vec{\Psi}$, the dual SH-ANM problem in (30) results in the identical solution Ω to following SDP

$$\begin{aligned} \min_{\mathbf{P},\Omega} \; & -\text{Re}\left\{\text{Tr}\left[\mathbf{R}^{\text{H}}\Omega\right]\right\} \\ \text{s.t.} \; & \text{Tr}(\Theta_{k,l}\tilde{\mathbf{G}}^{\text{H}}\mathbf{P}\tilde{\mathbf{G}}) = \delta_{k,l} \\ & k,\ l \in H \\ & \begin{bmatrix} \mathbf{P} & -\Omega^{\text{H}} \\ -\Omega & \mathbf{I} \end{bmatrix} \ge 0 \end{aligned} \tag{31}$$

if the maximum spherical harmonics order N is sufficiently high, where $\Theta_k \in \mathbb{R}^{(2N+1)\times(2N+1)}$ denotes the matrix with zeros except ones on the kth diagonal, $\Theta_{k,l} = \Theta_l \otimes \Theta_k$, $\delta_{k,l}$ is the Kronecker Delta function and H is a half space that $k, l \in [-2N-1, 2N+1]$.

Proof: Observe that the objective of (31) and (30) are the same, we only need to show they share the identical feasible set.

Since

$$\begin{aligned} & \|\Omega\|_{\mathcal{A}}^* \le 1 \\ \Leftrightarrow\ & \mathbf{Y}(\Psi)\mathbf{B}^{\text{H}}\Omega^{\text{H}}\Omega\mathbf{B}\mathbf{Y}^{\text{H}}(\Psi) \le 1 \\ \Leftrightarrow\ & F(\Psi) = 1 - \mathbf{Y}(\Psi)\mathbf{B}^{\text{H}}\Omega^{\text{H}}\Omega\mathbf{B}\mathbf{Y}^{\text{H}}(\Psi) \ge 0, \end{aligned} \tag{32}$$

where $F(\Psi)$ is a real positive polynomial. Let $\mathbf{y} = [y_{0,0}, y_{1,-1}, \ldots, y_{N,N}] \in \mathbb{R}^{(N+1)^2}$, with $y_{n,m}$ denoting the real spherical harmonic $Y_{n,m}(\Psi)$ for $\Psi \in \Xi$, we have

$$\begin{aligned} F(\Psi) &= 1 - \mathbf{Y}(\Psi)\mathbf{B}^{\text{H}}\Omega^{\text{H}}\Omega\mathbf{B}\mathbf{Y}^{\text{H}}(\Psi) \\ &= \frac{1}{C_N}\sum_{n=0}^{N}\sum_{m=-n}^{n} y_{n,m}^2 - \sum_j \left(\sum_{n=0}^{N}\sum_{m=-n}^{n} \alpha_{n,m,j} y_{n,m}\right)^2 \\ &\triangleq f(\mathbf{y}) \end{aligned} \tag{33}$$

with $C_N = \sum_{n=0}^{N} \frac{(4n+1)}{4\pi}$.

Note that the spherical harmonic $y_{n,m}$ can be written as a homogeneous polynomial of $y_{1,0}, y_{1,1}$ and $y_{1,-1}$, i.e. $y_{n,m} = H_{n,m}(y_{1,0}, y_{1,1}, y_{1,-1})$. Thus we define some nonnegative polynomials

$$g_v(\mathbf{y}) = \begin{cases} \sum_{m=-n}^{n} y_{n,m}^2 - \frac{2n+1}{4\pi}, \ v = n+1, \\ \frac{2n+1}{4\pi} - \sum_{m=-n}^{n} y_{n,m}^2, \ v = n+N+2, \\ y_{n,m} - H_{n.m}(y_{1,0},\ y_{1,-1},\ y_{1,1}), \\ v = 2N+2+n^2+n+m+1, \\ H_{n,m}(y_{1,0},\ y_{1,-1},\ y_{1,1}) - y_{n,m}, \\ v = N^2+4N+3+n^2+n+m+1, \\ \text{where} \quad m = -n, \ldots, n \quad \text{and} \quad n = 0, \ldots, N \end{cases} \tag{34}$$

and the sets

$$\begin{aligned} \mathcal{M}(g) &= \left\{ P \in \mathbb{R}[\mathbf{y}] \,|\, P = s_0 + \sum_{v=1}^{\chi} g_v s_v,\ s_v \in \sum \mathbb{R}[\mathbf{y}]^2 \right\}, \\ \mathcal{D}(g) &= \left\{ \mathbf{y} \in \mathbb{R}^{(N+1)^2} \,\middle|\, g_v(\mathbf{y}) \ge 0,\ v = 1, 2, \cdots, \chi \right\} \end{aligned} \tag{35}$$

where $\chi = 2(N+1)^2 + 2N + 2$, $\mathbb{R}[\mathbf{y}]$ and $\sum \mathbb{R}[\mathbf{y}]^2$ denote the set of real polynomials and real sum of squares polynomials on $\mathbf{y}$ respectively.

Observe that the polynomials $g_i(\mathbf{y})$ defined in (34) state Unsold's theorem and the relationship between real spherical harmonics, which implies for any $\mathbf{y} \in \mathcal{D}(g)$, $\mathbf{y}$ determines a vector of spherical harmonics $\mathbf{Y}(\Psi)$ uniquely. Applying this and (32) gives $f(\mathbf{y}) \ge 0$ for any $\mathbf{y} \in \mathcal{D}(g)$.

Therefore, $\mathcal{M}(g)$ is a quadratic module, because of non-empty $\mathcal{D}(g)$ [41]. Using this and (34) gives

$$\sum_{n=0}^{N} \frac{2n+1}{4\pi} - \sum_{n=0}^{N}\sum_{m=-n}^{n} y_{n,m}^2 = \sum_{v=N+2}^{2N+2} g_v(\mathbf{y}) \cdot 1 \in \mathcal{M}(g), \tag{36}$$

and thus $\mathcal{M}(g)$ is Archimedean, followed by Corollary 5.1.14 in [41]. This means for any $\mathbf{y} \in \mathcal{D}(g)$, we have $f(\mathbf{y}) \in \mathcal{M}(g)$, i.e.

$$\begin{aligned} f(\mathbf{y}) &= s_0 + \sum_{v=1}^{\chi} g_v s_v, \\ &= s_0, s_v \in \sum \mathbb{R}[\mathbf{y}]^2, \end{aligned} \tag{37}$$

which implies $F(\Psi)$ is sum-of-squares of real spherical harmonics.

Strictly speaking, the result in (37) is based on the sum-of-squares relaxation of the polynomial as shown in [24]. For a given $\vec{\Psi}$, [24] provides a mechanism to determine the harmonic order for the sum-of-squares relaxation.

Therefore, given a sufficient large N, according to the Gram matrix representation of trigonometric polynomials [42], a positive semidefinite matrix $\mathbf{P} \ge 0$ is existed that

$$F(\Psi) \ge 0 \Leftrightarrow \begin{cases} \text{Tr}(\Theta_{k,l}\tilde{\mathbf{G}}^{\text{H}}\mathbf{P}\tilde{\mathbf{G}}) = \delta_{k,l}, \\ k,\ l \in H, \\ \begin{bmatrix} \mathbf{P} & -\Omega^{\text{H}} \\ -\Omega & \mathbf{I} \end{bmatrix} \ge 0. \end{cases} \tag{38}$$

By (38) and (32), we can conclude that

$$\|\Omega\|_{\mathcal{A}}^* \le 1 \Leftrightarrow \begin{cases} \text{Tr}(\Theta_{k,l}\tilde{\mathbf{G}}^{\text{H}}\mathbf{P}\tilde{\mathbf{G}}) = \delta_{k,l} \\ k,\ l \in H \\ \begin{bmatrix} \mathbf{P} & -\Omega^{\text{H}} \\ -\Omega & \mathbf{I} \end{bmatrix} \ge 0, \end{cases} \tag{39}$$

and thus (30) and (31) share the identical solution Ω. ■

To show the optimality of solution for the SH-ANM problem in (20), we have the following dual certificate.

Theorem 3: The optimal solution of SH-ANM problem in (20) gives the unique atomic decomposition which is identical to (12) if there exist a dual polynomial:

$$\mathbf{q}(\Psi) = \mathbf{Y}(\Psi)\mathbf{B}^{\text{H}}\Omega \tag{40}$$

Satisfying

$$\begin{cases} \mathbf{q}(\Psi_k) = \boldsymbol{\rho}_k, & \forall k = 1, 2, \ldots, K \\ \|\mathbf{q}(\Psi)\|_2 < 1, & \forall \Psi \neq \Psi_k \end{cases} \tag{41}$$

Proof: The proof is shown in Appendix A. ■

Now the proof of Theorem 1 can be accomplished. As shown in [37], for a given $\vec{\Psi}$, the dual polynomial with sufficiently high order satisfying Theorem 3 indeed exists. Followed by (37), this polynomial is with the sum-of-squares relaxation order, which can be denoted as N, and thus Theorem 2 holds. In this situation, the dual problem of (20) can be solved by SDP problem in (31) and yield the identical atomic decomposition with the ground truth. By utilizing the standard Largrangian analysis (derivation details can be found in Appendix B), the dual problem of (31) is (25), which implies that $\|\mathbf{R}\|_{\mathrm{T}} = \|\mathbf{R}\|_{\mathcal{A}}$, followed by strong duality.

Regarding the Theorem 2 and 3 above, we have the following remarks:

Remark 4: Both the SDP formulation in Theorem 2 and the one in [34] are developed for super resolution with the spherical manifold and they both are based on the sum-of-squares relaxation for the polynomial either. In particular, our method is with a low-dimensional SDP formulation.

Remark 5: The methods in [25] and Theorem 2 are both based on a semi-algebraic set constrained by nonnegative polynomials. In particular, we limit the semi-algebraic set as the space of spherical harmonic vectors in our work.

Remark 6: It is noted that whether the SH-ANM approach can retrieve atomic decomposition exactly and the proposed method can solve SH-ANM problem efficiently are both related to the capability of resolution. Similar with [34], we will demonstrate the capability of resolution via numerical simulation in Section VI. Furthermore, we also note that some recent progress for the super resolution without resolution threshold can be found in [43], [44].

C. SH-ANM WITH SIGNAL DENOISING

In this section, we step to noisy cases where $\mathbf{V} \neq 0$. The covariance matrix estimation is obtained by averaging over snapshots in practice that

$$\begin{aligned} \hat{\mathbf{R}} &= \frac{1}{J}\sum_{t=1}^{J} \mathbf{P}(t)\mathbf{P}^{\mathrm{H}}(t) \\ &= \tilde{\mathbf{G}}\tilde{\mathbf{D}}(\vec{\Psi})\mathbf{R}_s\mathbf{D}^{\mathrm{H}}(\vec{\Psi})\tilde{\mathbf{G}}^{\mathrm{H}} + \boldsymbol{\eta} \\ &= \bar{\mathbf{R}} + \boldsymbol{\eta} \end{aligned} \tag{42}$$

where $\boldsymbol{\eta}$ is the outlier caused by additional noise and the finite snapshots effect.

A natural way to deal with additional noise for sparse recovery problem is via regularization.

It is shown in [45] that for the known number of sources, the smallest fitting error ε should be the optimal choice as long as no false alarm is observed. To this end, the signal denoising problem via SH-ANM can written as

$$\begin{aligned} \min_{\mathbf{Q},\mathbf{M},\mathbf{R}} \ & \frac{1}{2\zeta^2}\mathrm{Tr}(\tilde{\mathbf{G}}S(\mathbf{Q})\tilde{\mathbf{G}}^{\mathrm{H}}) + \frac{1}{2}\mathrm{Tr}(\mathbf{M}) \\ \text{s.t.} \ & \begin{bmatrix} \tilde{\mathbf{G}}S(\mathbf{Q})\tilde{\mathbf{G}}^{\mathrm{H}} & \mathbf{R} \\ \mathbf{R}^{\mathrm{H}} & \mathbf{M} \end{bmatrix} \geq 0 \\ & \left\| \hat{\mathbf{R}} - \mathbf{R} \right\|_2^2 \leq \varepsilon^2 \end{aligned} \tag{43}$$

where $\varepsilon = \|\boldsymbol{\eta}\|_2$ is the optimal choice for the recovery of covariance matrix $\mathbf{R}$. Here, we argue that ε can be set of $\varepsilon = (N+1)^2\sigma^2$, followed by [46], where σ is estimated by the square root of the smallest eigenvalue of $\hat{\mathbf{R}}$.

V. APPLICATION TO DOA ESTIMATION

In previews section, we presented a low dimensional SDP algorithm based on spherical harmonic atomic norm minimization (SH-ANM) approach for gridless sparse signal recovery on the spherical manifolds, which may yield various applications in signal denoising, imaging and source localization. As an example, we demonstrate the proposed algorithm to DOA estimation of spherical sensors array in free space and room reverberation environment.

A. POINT SOURCE DOA ESTIMATION IN FREE SPACE

Point source model is quite common in various scenarios, such as radar, wireless communication and acoustics, which represents the wavefield as a sum of Diracs. With a far-field assumption, the point source DOA estimation of spherical array can be regarded as identifying atoms from measurements in SH domain, and hence can be implemented based on SH-ANM approach.

Our SH-ANM based DOA estimation method steps from the recovered covariance matrix

$$\tilde{\mathbf{R}}^{\star} = \tilde{\mathbf{G}}S(\tilde{\mathbf{Q}}^{\star})\tilde{\mathbf{G}}^{\mathrm{H}}, \tag{44}$$

where $\tilde{\mathbf{Q}}^{\star}$ is the optimal solution of (43).

To extract DOAs from the solution to SH-ANM method, i.e. (44), we show the following analysis.

According to Theorem 1, $(\mathbf{Q}^{\star}, \mathbf{M}^{\star})$ given by

$$\begin{aligned} S(\mathbf{Q}^{\star}) &= \sum_{k=1}^{K} c_k \mathbf{f}(\Psi_k)\mathbf{f}^{\mathrm{H}}(\Psi_k), \\ \mathbf{M}^{\star} &= \sum_{k=1}^{K} c_k \boldsymbol{\rho}_k \boldsymbol{\rho}_k^{\mathrm{H}}, \end{aligned} \tag{45}$$

is one of the optimal solutions to the primal problem (25).

Note that the interior point methods found the solution with maximum rank since they searched the relative interior of the optimal face to obtain solution [47], which implies that interior point method results in the solution of (25) that spans the range space of the solution in (45). On the other hand, the objective function of (25) is the trace norm, which yields the solution of (25) with smaller rank.

Therefore, we argue that the principle component of $\tilde{\mathbf{R}}^{\star}$ spans the range space of (45), which motivates us to apply

the subspace method to the the recovered covariance matrix $\tilde{\mathbf{R}}^{\star}$ as

$$\tilde{\mathbf{R}}^{\star} = \mathbf{U}_s \Sigma_s \mathbf{U}_s^{\mathrm{H}} + \sigma^2 \mathbf{U}_N \mathbf{U}_N^{\mathrm{H}}. \tag{46}$$

The eigen-value decomposition of $\tilde{\mathbf{R}}^{\star}$ formulates the signal subspace $\mathbf{U}_s$ and noise subspace $\mathbf{U}_N$, and thus we have

$$\mathcal{R}(\mathbf{U}_s) \approx \mathcal{R}(\mathbf{B}\mathbf{Y}^{\mathrm{H}}(\vec{\Psi})) \tag{47}$$

where $\mathcal{R}(\mathbf{.})$ denotes the spanned subspace, so that SH-ESPRIT algorithm can be applied to $\mathbf{U}_s$ for 2-D DOA estimation.

Followed by the Legendre polynomial recurrence relationship, let

$$\begin{aligned}
\mathbf{D}_1 &= \mathrm{diag}\{\underbrace{0}_{n=1}, \underbrace{-1,0,1}_{n=2}, \ldots, \underbrace{-N+1,\ldots,N-1}_{n=N}\},\\
\mathbf{D}_2 &= \mathrm{diag}\{\underbrace{K^-_{1,0}}_{n=1}, \underbrace{K^-_{2,-1}, K^-_{2,0}, K^-_{2,1}}_{n=2}, \ldots, \underbrace{K^-_{N,-N+1},\ldots,K^-_{N,N-1}}_{n=N}\},\\
\mathbf{D}_3 &= \mathrm{diag}\{\underbrace{K^+_{1,0}}_{n=1}, \underbrace{K^+_{2,-1}, K^-_{2,0}, K^+_{2,1}}_{n=2}, \ldots, \underbrace{K^+_{N,-N+1},\ldots,K^+_{N,N-1}}_{n=N}\}
\end{aligned} \tag{48}$$

and

$$\mathbf{E} = [\mathbf{D}_2\mathbf{U}_s^{(-1)}\ \mathbf{D}_3\mathbf{U}_s^{(1)}], \tag{49}$$

where $K^{\pm}_{n,m} = \sqrt{(n \mp m)(n \pm m + 1)}$ and $\mathbf{U}_s^{(-1)}, \mathbf{U}_s^0, \mathbf{U}_s^{(1)}$ is generated from $\mathbf{U}_s$ as shown in [10], we have

$$\mathbf{D}_1\mathbf{U}_s^0 = \mathbf{E}\begin{bmatrix}\Delta^T\\ \Delta^H\end{bmatrix}, \tag{50}$$

then Δ can be solved as

$$\Delta = (\mathbf{E}^H\mathbf{E})^{-1}\mathbf{E}^H\mathbf{D}_1\mathbf{U}_s^0. \tag{51}$$

By computing the eigenvalues $u_k, k = 1,2,\ldots,K$, of Δ, we can obtain DOA of the kth source by $\hat{\theta}_k = \tan^{-1}|u_k|$ and $\hat{\varphi}_k = \arg(u_k)$ respectively.

B. SPEAKERS LOCALIZATION IN ROOM REVERBERATION ENVIRONMENT

Room reverberation induces the scenario with high correlated sources and underdetermined system, which degrade the performance of conventional DOA estimation method significantly. To deal with issues, the frequency diversity and the Time-Frequency sparsity of speech are exploited to address speakers localization problem in reverberation environment. In this work, we apply the SH-ANM approach for multiple speakers localization based on the Direct-Path Dominance (DPD) test [48]. The algorithm is consisted of four steps:

Firstly, we transform SH domain measurement data (8) into short time Fourier transform (STFT) domain as

$$\mathbf{P}_{\nu,\iota} = \mathbf{B}_\nu\mathbf{Y}^{\mathrm{H}}(\vec{\Psi})\mathbf{s}(\nu,\iota) + \mathbf{v}(\nu,\iota), \tag{52}$$

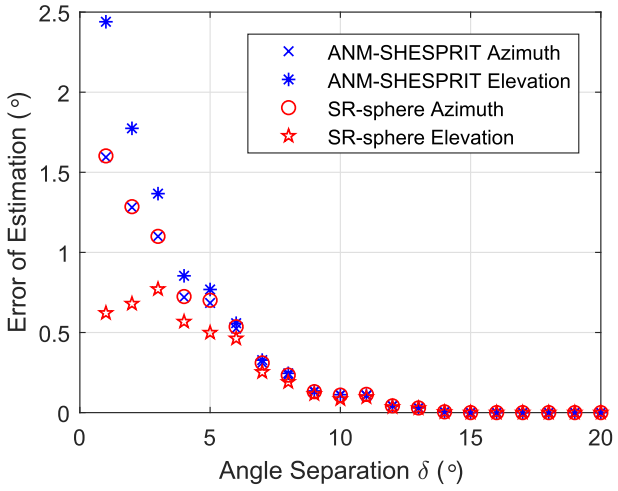

FIGURE 1. DOA Estimation error versus angular separation in noiseless single snapshot case.

and compute the local Time-Frequency (TF) covariance matrices in SH domain via frequency smoothing as

$$\hat{\mathbf{R}}(\nu,\iota) = \frac{1}{J_\nu J_\iota}\sum_{j_\nu=1}^{J_\nu}\sum_{j_\iota=1}^{J_\iota}\mathbf{B}_{\nu-j_\nu}^{-1}\mathbf{P}_{\nu-j_\nu,\iota-j_\iota}\mathbf{P}^{\mathrm{H}}_{\nu-j_\nu,\iota-j_\iota}(\mathbf{B}^{\mathrm{H}}_{\nu-j_\nu})^{-1}, \tag{53}$$

where ν and ι are the frequency and time index, $\mathbf{B}_\nu$ denotes the matrix $\mathbf{B}$ in (7) at frequency index ν.

Subsequently, DPD test is applied to the covariance matrices to identify TF-bins with the principle component on direct-path. The desired set of TF-bins is described as follows:

$$\mathcal{A}_{\mathrm{DPDtest}} = \left\{(\nu,\iota) : \frac{\sigma_1(\nu,\iota)}{\sigma_2(\nu,\iota)} > \zeta\right\} \tag{54}$$

with $\sigma_1(\nu,\iota)$ and $\sigma_2(\nu,\iota)$ the first and second largest eigenvalue of $\hat{\mathbf{R}}(\nu,\iota)$.

Assume that there is single dominant direct-path component in the selected TF-bins $(\nu,\iota) \in \mathcal{A}_{\mathrm{DPDtest}}$, the candidate DOAs of direct-path $\Psi_{\mathrm{TF}}(\nu,\iota)$ can be estimated by SH-ANM approach described in Section V-A.

Finally, we fusion the candidates of DOA estimation $\Psi_{\mathrm{TF}}(\nu,\iota)$ to establish the trajectories of speakers. Given the angle $\Psi^{(j)}_{\mathrm{TF}}(\nu,\iota)$ in jth sliding observation window of $\Psi_{\mathrm{TF}}(\nu,\iota)$, where the time index $\iota \in [\iota_j, \iota_j + \iota_{\mathrm{w}}]$ and the frequency index $\nu \in [\nu_{\mathrm{L}}, \nu_{\mathrm{H}}]$, we can calculate the spatial spectrum at $\Psi^{(j)}_{\mathrm{TF}}(\nu,\iota)$ in the window by

$$p(\nu,\iota) = \mathbf{Y}(\Psi^{(j)}_{\mathrm{TF}}(\nu,\iota))\mathbf{U}_n, \tag{55}$$

and choose DOAs $\Psi_i, i = 1,\ldots,q$ corresponding to the q highest peaks as the centers for clustering.

Define the distance between the clustering center $\Psi_i = (\theta_i, \phi_i)$ and a certain DOA $\Psi_{\mathrm{TF}} = (\theta_{\mathrm{TF}}, \phi_{\mathrm{TF}})$ in the

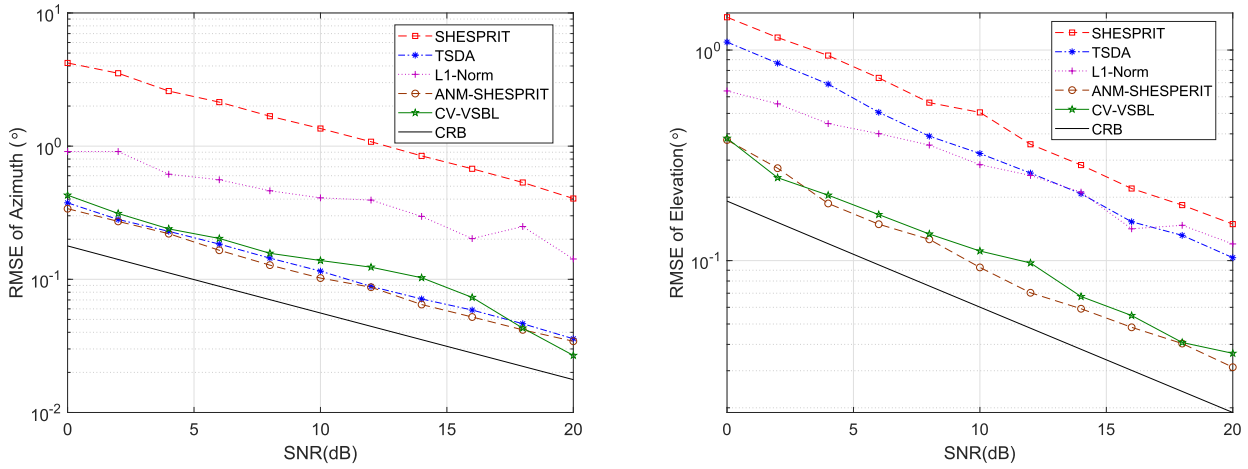

FIGURE 2. Performance comparison under different SNRs for uncorrelated sources at $(\theta, \varphi) = (20°, 50°), (30°, 120°)$, $L = 200$ when SNR varies from 0 to 20dB.

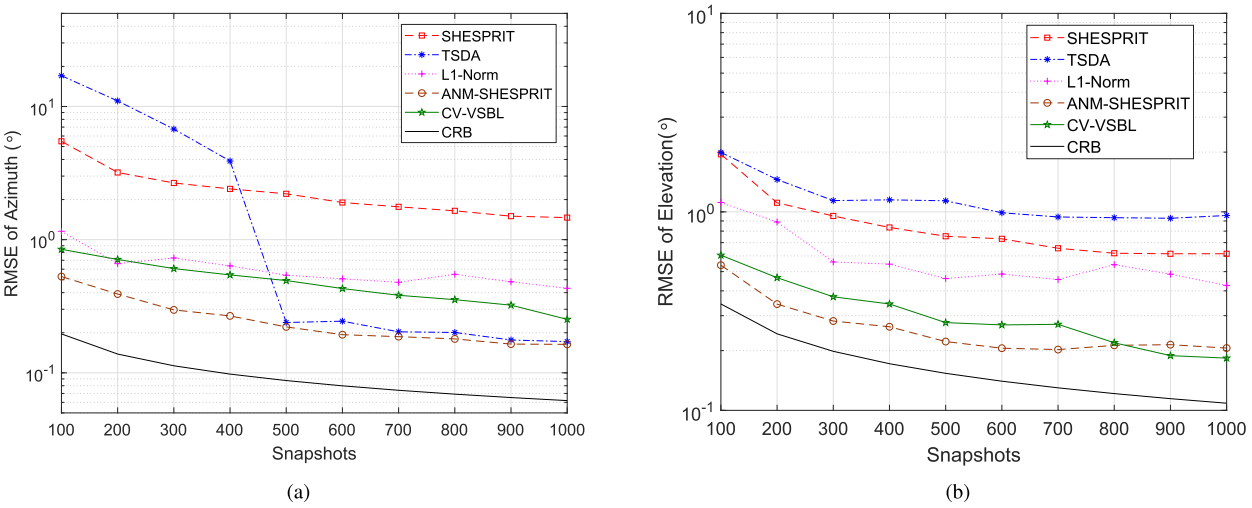

FIGURE 3. Performance comparison with various number of snapshots for uncorrelated sources at $(\theta, \varphi) = (20°, 50°), (26°, 128°)$, SNR = 0dB.

observation window $\Psi_{\mathrm{TF}}^{(j)}(\nu, \iota)$ as

$$d(\Psi_i, \Psi_{\mathrm{TF}}) = \cos^{-1}(\cos\theta_{\mathrm{TF}} \cos\theta_i + \cos(\phi_{\mathrm{TF}} - \phi_i) \sin\theta_{\mathrm{TF}} \sin\theta_i), \quad (56)$$

we list and sort the count of the elements in the set

$$\mathcal{B}_i = \left\{ \Psi_{\mathrm{TF}}(\nu, \iota) : d(\Psi_i, \Psi_{\mathrm{TF}}) < 10° \right\}, \quad (57)$$

and pick up $\mathcal{B}_i$ with the highest count as the first cluster and removed from the sorted list. If the next set $\mathcal{B}_j$ satisfying $d(\Psi_i, \Psi_j) < 10°$, the set $\mathcal{B}_j$ is removed from the list and combined into the existed cluster, otherwise establish a new cluster. Repeat the procedure till all candidates in the list are clustered. The DOAs of speakers in such frame can be obtained via Gaussian-Mixed Model(GMM) cluster by cluser.

The efficacy of the algorithm proposed in Section V-A and V-B will be verified with simulations and real-life measurements data in Section VI and VII, respectively.

VI. SIMULATIONS

This section evaluates the DOA estimation performance of proposed method in Section V-A for point sources in free space through simulations.

Firstly, we demonstrate the capability of resolution to SH-ANM method and the super resolution method on the sphere in [34] for single snapshot and noiseless case. Then, the comparison of the DOA estimation performance in noisy case between SH-ANM method in Section V-A and l_1 norm based method in [16], the SHESPRIT in [10], TSDA (estimate elevations with U-SHESPRIT and estimate azimuths with U-SHRMUSIC) in [11], CV-VSBL in [17] and Cramer-Rao Bound (CRB) in [49] is presented. Here, we refer

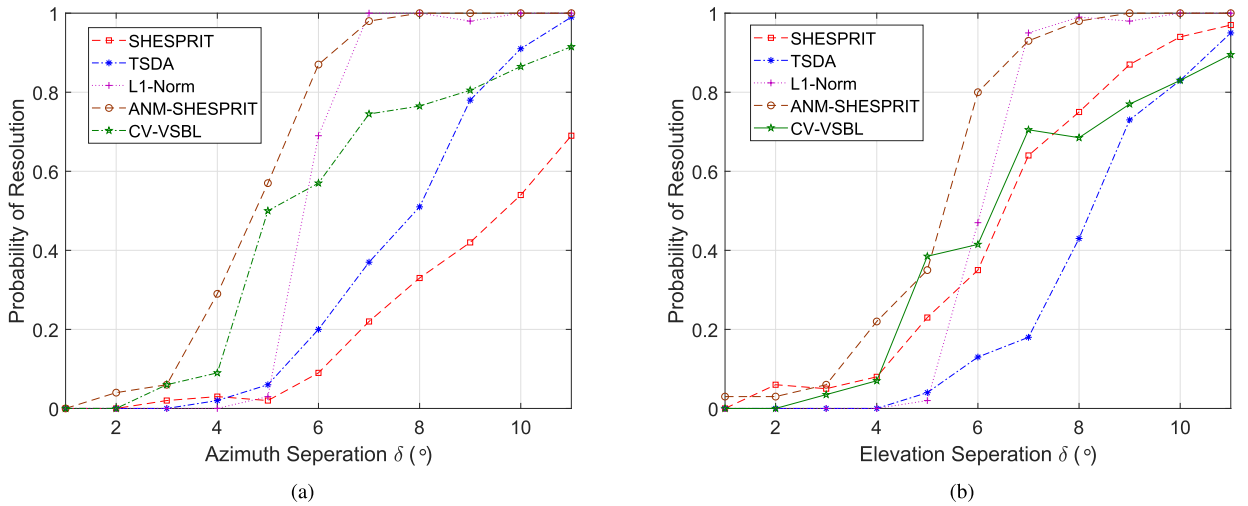

FIGURE 4. Probability of resolution versus angular separation for uncorrelated sources at $(\theta, \varphi) = (30°, 50°)$, $(30° + \delta, 50° + \delta)$, SNR = 3dB.

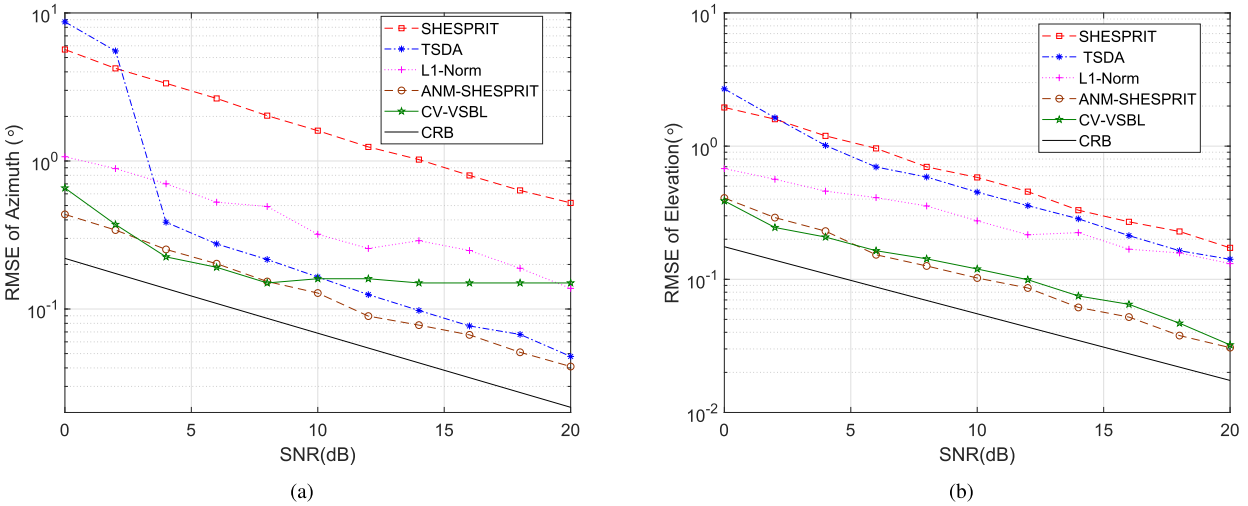

FIGURE 5. Performance comparison with different SNRs for correlated sources $(\theta, \varphi) = (20°, 50°)$, $(30°, 120°)$, $L = 200$, $\alpha = 0.6$.

to the SH-ANM method with SH-ESPRIT in Section V-A as ANM-SHESPRIT.

All the simulations are carried out on the order $N = 4$ rigid spherical array with 38 sensors followed by Lebedev distribution [50]. The radius of spherical array is $r = 0.042$m and the signals are narrowband AM signals with $2\pi r/\lambda = 2.7$ to avoid the spatial aliasing. The discretion sparsity based methods estimates DOAs by searching the K largest peaks of the spectrum with the 0.2° grid interval (unless otherwise specified). As a metric of performance, RMSE is utilized to algorithm evaluation as

$$\text{RMSE}=\sqrt{\frac{1}{MK}\sum_{i=1}^{K}\sum_{j=1}^{M}(\widehat{\theta}_{ij}-\theta_i)^2} \tag{58}$$

with the simulation trials number M and the source number K. $\widehat{\theta}_{ij}$ and θ_i denote the estimation and the ground truth of the ith DOA at jth trial. For each simulation, 200 Monte Carlo trials are performed using PC with Intel i7-8700K, 3.7GHz and 6GB memory.

A. COMPARISON OF RESOLUTION CAPABILITY

Suppose that two sources locate at $(\theta, \varphi) = (30°, 50°)$ and $(30°+\delta, 50°+\delta)$, and the angle separation δ varies from 1° to 20°. We refer to the super resolution on the sphere method in [34] as SR-Sphere and compare the average DOA estimation error of ANM-SHESPRIT method and SR-Sphere method in noiseless single snapshot case. The signals are the complex random data with equal power. Fig. 1 shows the average estimation error of 200 trails varus angle separation. We can see that the two methods have the similar DOA estimation error which implies they may have almost the identical capability of resolution. To evaluate the computational complexity, we compute the average time per trail of the two methods.

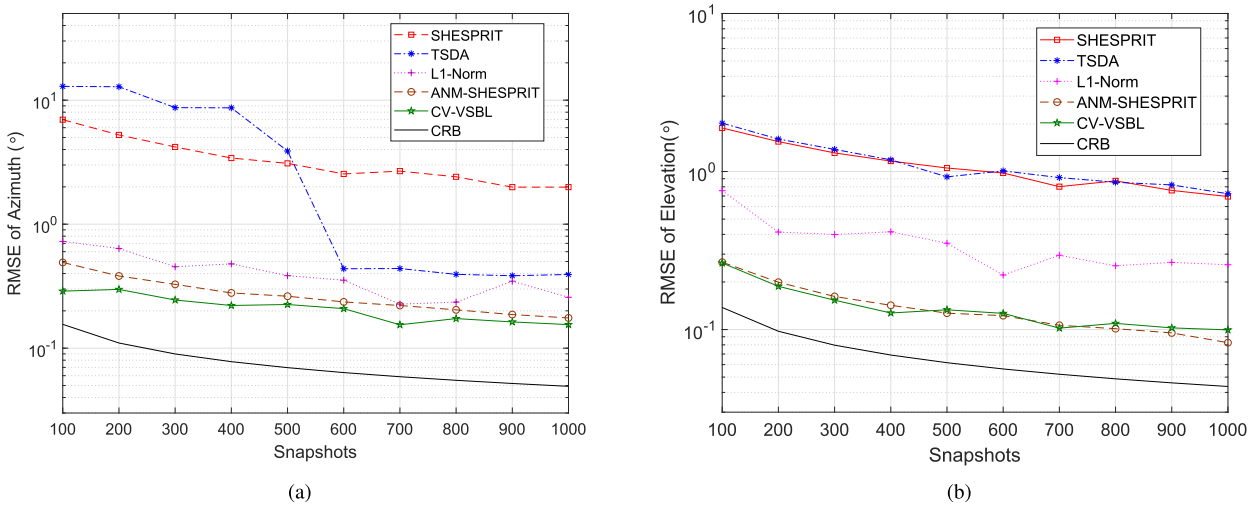

FIGURE 6. Performance comparison with various numbers of snapshots for correlated sources at $(\theta, \varphi) = (20°, 50°), (26°, 128°)$, $\alpha = 0.7$, SNR = 5dB.

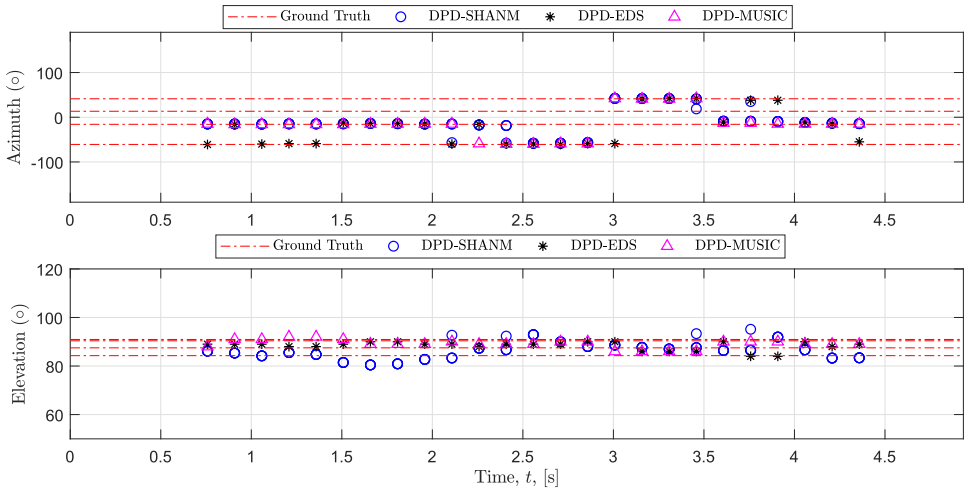

FIGURE 7. Estimated DOAs as a function of time with the DPD-SHANM, DPD-MUSIC and DPD-EDS method for Task 2 Recording 2 in LOCATA challenge.

Our method takes 0.4388s average per trail and SR-sphere method takes 1.2626s average per trail respectively, which indicates that our method is more computational efficient.

B. PERFORMANCE FOR UNCORRELATED SOURCES

We compare SH-ANM based method with some baselines for uncorrelated sources. In this example, there are two equal-power independent sources impinging onto the spherical array from$(\theta, \varphi) = (20°, 50°)$ and $(30°, 120°)$. We use 200 snapshots in each trail and SNR level varies from 20 to 0 dB.

Fig. 2 shows the RMSE of TSDA, ANM-SHESPRIT, CV-VSBL and SHESPRIT methods. For azimuth estimation ANM-SHESPRIT provides similar accuracy with TSDA method and performs better for elevation estimation however. Furthermore, our method shows the superior performance compared to the other algorithms. Note that L1-norm based method exhibits poorest performance among sparsity based methods. This is probably due to the difficulty on the choice of regularization parameter and the effects to the truncating SVD processing.

Next, we present the comparison of the algorithms versus different number of snapshots with fixed SNR at 0dB. The two uncorrelated sources are located at $(\theta, \varphi) = (20°, 50°)$ and $(26°, 128°)$.

It is indicated in Fig.3 that the ANM-SHESPRIT demonstrates the best performance.

Then we compare the resolution probability of the ANM-SHESPRIT with L1-Norm, SHESPRIT, CV-VSBL and TSDA method versus angle separation. The grid interval is 1° and SNR is fixed at 3dB. Suppose two uncorrelated sources are at $(\theta, \varphi) = (30°, 50°)$ and $(30° + \delta, 50° + \delta)$, we assume the elevation of the two signals to be resolved

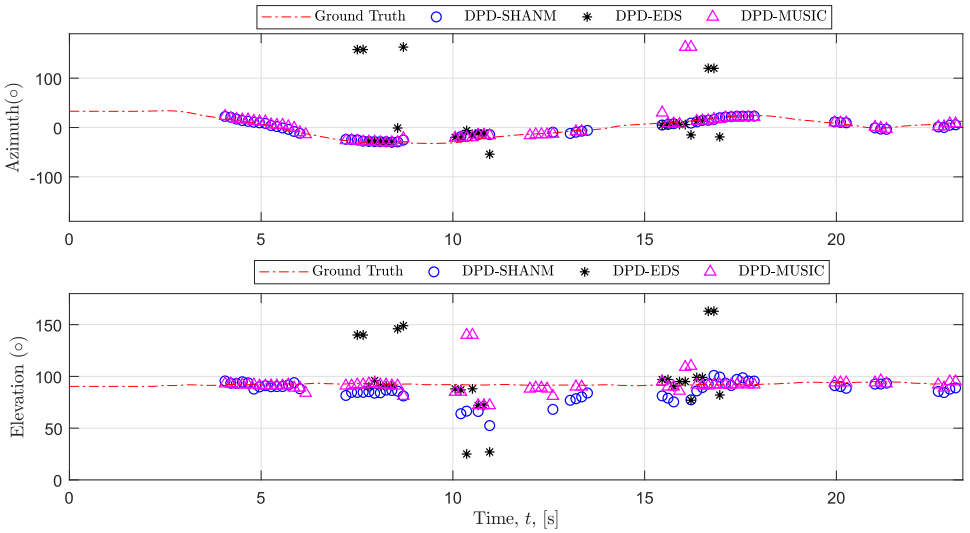

FIGURE 8. Estimated DOAs as a function of time with the DPD-SHANM, DPD-MUSIC and DPD-EDS method for Task 3 Recording 1 in LOCATA challenge.

successfully that both $\left|\hat{\theta}_1 - \theta_1\right|$ and $\left|\hat{\theta}_2 - \theta_2\right|$ are less than $|\theta_1 - \theta_2|/2$, and the resolution probability of azimuth can be defined similarly.

The ANM-SHESPRIT method outperforms the other methods as shown in Fig. 4, and thus exhibits super resolution capability of proposed method to DOA estimation.

C. PERFORMANCE FOR CORRELATED SOURCES

In this section, we investigate robustness of algorithms to correlated sources. The locations of two sources are the same as the simulations shown in Fig.2 with the signal correlation coefficient of $\alpha = 0.6$ and 200 snapshots. The RMSE simulation results of the different methods versus SNR are shown in Fig.5.

It is shown that for the correlated sources, all subspace based methods suffer the performance degradation compared in uncorrelated sources case, but the ANM-SHESPRIT method shows robust to correlated signals. For azimuth estimation case, the ANM-SHESPRIT method can achieve best accuracy among these methods when SNR varies from 10dB to 20dB. And for elevation estimation, ANM-SHESPRIT method is also satisfactory.

Fig.6 demonstrates the RMSE of our method, L1-Norm, SHESPRIT and TSDA method versus number of snapshots, where we assume two correlated sources located at $(\theta, \varphi) = (20°, 50°)$ and $(26°, 128°)$ with correlation coefficient of $\alpha = 0.7$ and SNR $= 5$ dB. Results reveals that ANM-SHESPRIT method provides robustness to highly correlated sources.

VII. EXPERIMENTS

In this section, we verify the algorithm proposed in section V-B with real recording from LOCATA challenge [35], which presents several acoustics scenarios in a lecture room at Hulboldt University Berlin. Here, we consider two of the tasks from the challenge for multiple static loudspeakers (Task 2) and single moving speaker (Task 3) using Eigenmike spherical microphone array. The proposed method in Section V-B is referred to as DPD-SHANM and compare its performance with DPD-MUSIC [48] and DPD-EDS [51].

The sample frequency of the recorded signals is 48kHz and we choose a Hamming window of 1024 samples with 75% overlap for STFT transformation. The SH order is $N = 3$ and the processing frequency band is 1000-3000Hz. The length and bandwidth of a frame for frequency smoothing in (53) are $J_\nu = 15$ and $J_\iota = 15$ and the length of slide window for trajectories fusion is $\iota_{\mathrm{w}} = 10$ (about 0.25s). The ratio ζ for DPD test is set to 2. The array calibration was carried out as mentioned in [51].

For the multiple static sources localization task, the recording 2 in task 2 of the challenge is used to evaluate the algorithms, and the results of localization and tracking are shown in Fig. 7. The results of the single moving speaker tracking is presented in Fig. 8. We can see that the estimates of moving speakers are perturbated more seriously than the static loudspeaker scene but the proposed method has fewer estimation outliers than the counterparts.

VIII. CONCLUSION

We study the gridless sparse signal representation problem for the signal on the spherical manifolds, where the signals are composed of a combination of the vectors of spherical harmonics, with the application to DOA estimation of spherical array in this paper. An covariance matrix based SH-ANM approach is proposed with a low-dimensional SDP implementation. We also develop SH-ANM based DOA estimation method for free space and room reverberation environment. As shown in simulated results, the SH-ANM based method presents the enhancement of performance in various scenarios compared with conventional techniques. Finally the

experiments with LOCATA challenge recordings verify the superiority of the SH-ANM based method.

APPENDIX A
PROOF OF THEOREM 3

Since any Ω satisfying (41) is dual feasible, it gives

$$\begin{aligned}\|\mathbf{R}\|_{\mathcal{A}} &\geq \|\mathbf{R}\|_{\mathcal{A}}\|\Omega\|_{\mathcal{A}}^{*} \geq \mathrm{Re}\left\{\mathrm{Tr}(\mathbf{R}\Omega^{\mathrm{H}})\right\} \\ &= \mathrm{Re}\left\{\mathrm{Tr}(\sum_{k=1}^{K} c_k \mathbf{B}\mathbf{Y}^{\mathrm{H}}(\Psi_k)\boldsymbol{\rho}_k\Omega^{\mathrm{H}})\right\} \\ &= \sum_{k=1}^{K}\mathrm{Re}\left\{c_k\mathrm{Tr}(\Omega^{\mathrm{H}}\mathbf{B}\mathbf{Y}^{\mathrm{H}}(\Psi_k)\boldsymbol{\rho}_k)\right\} \\ &= \sum_{k=1}^{K}\mathrm{Re}\left\{c_k\mathrm{Tr}(\boldsymbol{\rho}_k^{\mathrm{H}}\boldsymbol{\rho}_k)\right\} = \sum_{k=1}^{K} c_k \geq \|\mathbf{R}\|_{\mathcal{A}}. \end{aligned} \tag{59}$$

Thus, $\mathrm{Re}\left\{\mathrm{Tr}(\mathbf{R}\Omega^{\mathrm{H}})\right\} = \|\mathbf{R}\|_{\mathcal{A}}$. By strong duality, we have the atomic decomposition in (12) is optimal to (20) and Ω is dual optimal.

To show the uniqueness, given $\mathbf{R}$ has another optimal atomic decomposition that

$$\begin{aligned}\mathbf{R} &= \sum_{k=1}^{K} c_k \mathbf{B}\mathbf{Y}^{\mathrm{H}}(\Psi_k)\boldsymbol{\rho}_k \\ &= \mathbf{R} + \sum_{k=1}^{K} c_k' \mathbf{B}\mathbf{Y}^{\mathrm{H}}(\Psi_k)\boldsymbol{\rho}_k' + \sum_{l=1}^{L} c_l \mathbf{B}\mathbf{Y}^{\mathrm{H}}(\Psi_l)\boldsymbol{\rho}_l. \end{aligned} \tag{60}$$

where $c_k, c_k', c_l > 0$, the set $\{\Psi_k\}\bigcap\{\Psi_l\} = \emptyset$. By (40) and (41), there exists Ω' that

$$\begin{cases}\mathbf{q}'(\Psi_k) = \boldsymbol{\rho}_k', & \forall k = 1, 2, \ldots, K \\ \left\|\mathbf{q}'(\Psi)\right\|_2 < 1, & \forall \Psi \neq \Psi_k \end{cases} \tag{61}$$

with $\mathbf{q}'(\Psi) = \mathbf{Y}(\Psi)\mathbf{B}^{\mathrm{H}}\Omega'$. It implies

$$\sum_{k=1}^{K} c_k' + \mathrm{Tr}\{\sum_{l=1}^{L} c_l \Omega'^{\mathrm{H}}\mathbf{B}\mathbf{Y}^{\mathrm{H}}(\Psi_l)\boldsymbol{\rho}_l\} = 0 \tag{62}$$

and

$$\sum_{l=1}^{L} c_l > |\mathrm{Tr}\{\sum_{l=1}^{L} c_l \Omega'^{\mathrm{H}}\mathbf{B}\mathbf{Y}^{\mathrm{H}}(\Psi_l)\boldsymbol{\rho}_l\}|, \tag{63}$$

thus

$$\sum_{l=1}^{L} c_l > \sum_{k=1}^{K} c_k'. \tag{64}$$

We then have

$$\begin{aligned}\|\mathbf{R}\|_{\mathcal{A}} &\geq \sum_{l=1}^{L} c_l + \sum_{k=1}^{K}(c_k' + c_k) \\ &\geq \sum_{k=1}^{K} c_k + \sum_{l=1}^{L} c_l - \sum_{k=1}^{K} c_k' \\ &> \sum_{k=1}^{K} c_k = \|\mathbf{R}\|_{\mathcal{A}}, \end{aligned} \tag{65}$$

which is a contradiction. Hence, $\mathbf{R} = \sum_{k=1}^{K} c_k \mathbf{B}\mathbf{Y}^{\mathrm{H}}(\Psi_k)\boldsymbol{\rho}_k$ is the unique solution of (20).

APPENDIX B
DERIVATION OF DUAL PROBLEM OF (31)

Let $\Lambda = \begin{bmatrix}\mathbf{S} & \mathbf{Z} \\ \mathbf{Z}^{\mathrm{H}} & \mathbf{M}\end{bmatrix} \geq 0$ and $\mathbf{Q}$ be the Largrangian multipliers of the two constraints of (25), the Largrangian function of (25) can be given as

$$\begin{aligned}&L(\mathbf{Q}, \mathbf{M}, \mathbf{S}, \mathbf{Z}) \\ &= -\mathrm{Re}\left\{\mathrm{Tr}(\mathbf{R}\Omega^{\mathrm{H}})\right\} + \sum_{k,l\in H} q_{k,l}(\mathrm{Tr}(\Theta_{k,l}\tilde{\mathbf{G}}^{\mathrm{H}}\mathbf{P}\tilde{\mathbf{G}}) - \delta_{k,l}) \\ &\quad -\mathrm{Tr}\left\{\begin{bmatrix}\mathbf{P} & -\Omega \\ -\Omega^{\mathrm{H}} & \mathbf{I}\end{bmatrix}\Lambda\right\} \\ &= -\frac{1}{2}\mathrm{Tr}(\mathbf{R}\Omega^{\mathrm{H}} + \Omega\mathbf{R}^{\mathrm{H}}) - \mathrm{Tr}(\mathbf{P}\mathbf{S} - \Omega\mathbf{Z}^{\mathrm{H}} - \Omega^{\mathrm{H}}\mathbf{Z} + \mathbf{M}) \\ &\quad + \sum_{k,l\in H} q_{k,l}(\mathrm{Tr}(\Theta_{k,l}\tilde{\mathbf{G}}^{\mathrm{H}}\mathbf{P}\tilde{\mathbf{G}}) - \mathrm{Tr}(\Theta_{k,l}\tilde{\mathbf{G}}^{\mathrm{H}}\tilde{\mathbf{G}})/\zeta^2). \end{aligned} \tag{66}$$

which is followed by $\mathrm{Tr}(\Theta_{k,l}\tilde{\mathbf{G}}^{\mathrm{H}}\tilde{\mathbf{G}})/\zeta^2 = \delta_{k,l}$.

For minimizing $L(\mathbf{Q}, \mathbf{M}, \mathbf{S}, \mathbf{Z})$, we can partial derivate to $L(\mathbf{Q}, \mathbf{M}, \mathbf{S}, \mathbf{Z})$ with respect to $(\mathbf{P}, \Omega)$ which results that

$$\begin{cases}\mathbf{S} = \tilde{\mathbf{G}}\left[\sum_{k,l\in H} q_{k,l}\Theta_{k,l}\right]\tilde{\mathbf{G}}^{\mathrm{H}}, \\ \frac{1}{2}\mathbf{R} = \mathbf{Z}, \end{cases} \tag{67}$$

and thus it gives

$$\inf(L) = -\mathrm{Tr}(\tilde{\mathbf{G}}S(\mathbf{Q})\tilde{\mathbf{G}}^{\mathrm{H}})/\zeta^2 - \mathrm{Tr}(\mathbf{M}). \tag{68}$$

Then the dual problem of (31) is

$$\begin{aligned}&\min_{\mathbf{Q},\mathbf{M}} \frac{1}{\zeta^2}\mathrm{Tr}(\tilde{\mathbf{G}}S(\mathbf{Q})\tilde{\mathbf{G}}^{\mathrm{H}}) + \mathrm{Tr}(\mathbf{M}) \\ &\text{s.t.} \quad \begin{bmatrix}\tilde{\mathbf{G}}S(\mathbf{Q})\tilde{\mathbf{G}}^{\mathrm{H}} & \frac{1}{2}\mathbf{R} \\ \frac{1}{2}\mathbf{R}^{\mathrm{H}} & \mathbf{M}\end{bmatrix} \geq 0, \end{aligned} \tag{69}$$

which is equivalent to

$$\begin{aligned}&\min_{\mathbf{Q},\mathbf{M}} \frac{1}{2\zeta^2}\mathrm{Tr}(\tilde{\mathbf{G}}S(\mathbf{Q})\tilde{\mathbf{G}}^{\mathrm{H}}) + \frac{1}{2}\mathrm{Tr}(\mathbf{M}) \\ &\text{s.t.} \quad \begin{bmatrix}\tilde{\mathbf{G}}S(\mathbf{Q})\tilde{\mathbf{G}}^{\mathrm{H}} & \mathbf{R} \\ \mathbf{R}^{\mathrm{H}} & \mathbf{M}\end{bmatrix} \geq 0. \end{aligned} \tag{70}$$

Therefore, the dual problem of (31) is (25).

REFERENCES

[1] E. Levin, T. Bendory, N. Boumal, J. Kileel, and A. Singer, "3D ab *initio* modeling in cryo-EM by autocorrelation analysis," 2017, *arXiv:1710.08076*. [Online]. Available: https://arxiv.org/abs/1710.08076

[2] M. Costa, A. Richter, and V. Koivunen, "Unified array manifold decomposition based on spherical harmonics and 2-D Fourier basis," *IEEE Trans. Signal Process.*, vol. 58, no. 9, pp. 4634–4645, Sep. 2010.

[3] B. Rafaely, "Analysis and design of spherical microphone arrays," *IEEE Trans. Speech Audio Process.*, vol. 13, no. 1, pp. 135–143, Jan. 2015.

[4] G. Zheng, "Doa estimation in MIMO radar with non-perfectly orthogonal waveforms," *IEEE Commun. Lett.*, vol. 2, no. 21, pp. 414–417, Oct. 2017.

[5] F. Wen, X. Zhang, F. Yang, and Z. Zhang, "Direction finding in bistatic MIMO radar with unknown spatially colored noise," in *Proc. IEEE 23rd Int. Conf. Digit. Signal Process.*, Nov. 2018, pp. 1–5. doi: 10.1109/ICDSP.2018.8631628.

[6] Z. D. Zheng and J. Y. Zhang, "Fast method for multi-target localisation in bistatic MIMO radar," *Electron. Lett.*, vol. 47, no. 2, pp. 138–139, 2011.

[7] B. Tang, J. Tang, Y. Zhang, and Z. Zheng, "Maximum likelihood estimation of DOD and DOA for bistatic MIMO radar," *Signal Process.*, vol. 93, no. 5, pp. 1349–1357, 2013.

[8] F. Wen, C. Mao, and G. Zhang, "Direction finding in MIMO radar with large antenna arrays and nonorthogonal waveforms," *Digital Signal Process.*, vol. 94, pp. 75–83, Nov. 2019. doi: 10.1016/j.dsp.2019.06.008.

[9] Q. Huang, L. Xiang, Y. Fang, and G. Zhang, "Unitary transformations for spherical harmonics MUSIC," *Signal Process.*, vol. 131, pp. 441–446, Feb. 2017.

[10] R. Goossens and R. Rogier, "Closed-form 2D angle estimation with a spherical array via spherical phase mode excitation and esprit," in *Proc. IEEE Int. Conf. Acoust., Speech Signal Process. (ICASSP)*, Mar./Apr. 2008, pp. 2321–2324.

[11] Q. Huang, Y. Fang, and L. Zhang, "Two-stage decoupled DOA estimation based on real spherical harmonics for spherical arrays," *IEEE/ACM Trans. Audio, Speech, Language Process.*, vol. 25, no. 11, pp. 2045–2058, Nov. 2017.

[12] B. Liao, "Fast angle estimation for MIMO radar with nonorthogonal waveforms," *IEEE Trans. Aerosp. Electron. Syst.*, vol. 54, no. 4, pp. 2091–2096, Aug. 2018.

[13] H. Wang, L. Wan, M. Dong, K. Ota, and X. Wang, "Assistant vehicle localization based on three collaborative base stations via SBL-based robust DOA estimation," *IEEE Internet Things J.*, vol. 6 no. 3, pp. 5766–5777, Jun. 2019.

[14] H. Rauhut and R. Ward, "Sparse recovery for spherical harmonic expansions," 2011, *arXiv:1102.4097*. [Online]. Available: https://arxiv.org/abs/1102.4097

[15] N. Burq, S. Dyatlov, R. Ward, and M. Zworski, "Weighted eigenfunction estimates with applications to compressed sensing," *SIAM J. Math. Anal.*, vol. 44, no. 5, pp. 3481–3501, Jan. 2012.

[16] P. K. T. Wu, C. Jin, and N. Epain, "A dereverberation algorithm for spherical microphone arrays using compressed sensing techniques," in *Proc. IEEE Int. Conf. Acoust., Speech Signal Process. (ICASSP)*, Mar. 2012, pp. 4053–4056.

[17] Q. Huang, G. Zhang, and Y. Fang, "Real-valued DOA estimation for spherical arrays using sparse Bayesian learning," *Signal Process.*, vol. 125, pp. 79–86, Aug. 2016.

[18] W. Dai and H. Chen, "Multiple speech sources localization in room reverberant environment using spherical harmonic sparse Bayesian learning," *IEEE Sensors Lett.*, vol. 3, no. 2, Feb. 2019, Art. no. 7000304.

[19] Q. Huang, L. Kai, and L. Xiang, "Off-grid DOA estimation in real spherical harmonics domain using sparse Bayesian inference," *Signal Process.*, vol. 137, pp. 124–134, Aug. 2017.

[20] V. Chandrasekaran, B. Recht, P. A. Parrilo, and A. S. Willsky, "The convex geometry of linear inverse problems," *Found. Comput. Math.*, vol. 12, pp. 805–849, Dec. 2012.

[21] E. J. Candès and C. Fernandez-Granda, "Towards a mathematical theory of super-resolution," *Commun. Pure Appl. Math.*, vol. 67, no. 6, pp. 906–956, Jun. 2014.

[22] Y. Chi and Y. Chen, "Compressive two-dimensional harmonic retrieval via atomic norm minimization," *IEEE Trans. Signal Process.*, vol. 63, no. 4, pp. 1030–1042, Feb. 2015.

[23] Z. Yang, L. Xie, and P. Stoica, "Vandermonde decomposition of multilevel toeplitz matrices with application to multidimensional super-resolution," *IEEE Trans. Inf. Theory*, vol. 62, no. 6, pp. 3685–3701, Jun. 2016.

[24] W. Xu, J.-F. Cai, K. V. Mishra, M. Cho, and A. Kruger, "Precise semidefinite programming formulation of atomic norm minimization for recovering D-dimensional ($D \geq 2$) off-the-grid frequencies," in *Proc. Inf. Theory Appl. Workshop (ITA)*, San Diago, CA, USA, Feb. 2014, pp. 1–4.

[25] K. V. Mishra, M. Cho, A. Kruger, and W. Xu, "Spectral super-resolution with prior knowledge," *IEEE Trans. Signal Process.*, vol. 63, no. 20, pp. 5342–5357, Oct. 2015.

[26] Y. Li and Y. Chi, "Off-the-grid line spectrum denoising and estimation with multiple measurement vectors," *IEEE Trans. Signal Process.*, vol. 64, no. 5, pp. 1257–1269, Mar. 2016.

[27] Z. Yang, L. Xie, and C. Zhang, "A discretization-free sparse and parametric approach for linear array signal processing," *IEEE Trans. Signal Process.*, vol. 62, no. 19, pp. 4959–4973, Oct. 2014.

[28] X. Wu, W.-P. Zhu, and J. Yan, "A Toeplitz covariance matrix reconstruction approach for direction-of-arrival estimation," *IEEE Trans. Veh. Technol.*, vol. 66, no. 9, pp. 8223–8237, Sep. 2017.

[29] C. Steffens, M. Pesavento, and M. E. Pfetsch, "A compact formulation for the $\ell_{2,1}$ mixed-norm minimization problem," *IEEE Trans. Signal Process.*, vol. 66, no. 6, pp. 1483–1497, Mar. 2018.

[30] T. Bendory, S. Dekel, and A. Feuer, "Exact recovery of Dirac ensembles from the projection onto spaces of spherical harmonics," *Constructive Approximation*, vol. 24, no. 2, pp. 183–207, 2015.

[31] F. Roemer, S. Semper, T. Hotz, and G. D. Galdo, "Grid-free direction-of-arrival estimation with compressed sensing and arbitrary antenna arrays," in *Proc. IEEE Int. Conf. Acoust., Speech Signal Process. (ICASSP)*, Apr. 2018, pp. 3251–3255.

[32] K. Mahata and M. M. Hyder, "Grid-less T.V minimization for DOA estimation," *Signal Process.*, vol. 132, pp. 155–164, Mar. 2017.

[33] K. Mahata and M. M. Hyder, "Fast frequency estimation with prior information," *IEEE Trans. Signal Process.*, vol. 66, no. 1, pp. 264–273, Jan. 2018.

[34] T. Bendory, S. Dekel, and A. Feuer, "Super-resolution on the sphere using convex optimization," *IEEE Trans. Signal Process.*, vol. 63, no. 9, pp. 2253–2262, May 2015.

[35] H. W. Löllmann, C. Evers, A. Schmidt, H. Mellmann, H. Barfuss, P. A. Naylor, and W. Kellermann, "The LOCATA challenge data corpus for acoustic source localization and tracking," in *Proc. IEEE Sensor Array Multichannel Signal Process. Workshop (SAM)*, Sheffield, U.K., Jul. 2018, pp. 410–414.

[36] J. Yin and T. Chen, "Direction-of-arrival estimation using a sparse representation of array covariance vectors," *IEEE Trans. Signal Process.*, vol. 59, no. 9, pp. 4489–4493, Sep. 2011.

[37] G. Tang, B. N. Bhaskar, P. Shah, and B. Recht, "Compressed sensing off the grid," *IEEE Trans. Inf. Theory*, vol. 59, no. 11, pp. 7465–7490, Nov. 2013.

[38] C.-Y. Hung and M. Kaveh, "Direction-finding based on the theory of super-resolution in sparse recovery algorithms," in *Proc. IEEE Int. Conf. Acoust., Speech Signal Process. (ICASSP)*, Apr. 2015, pp. 2404–2408.

[39] Z. Yang and L. Xie, "Enhancing sparsity and resolution via reweighted atomic norm minimization," *IEEE Trans. Signal Process.*, vol. 64, no. 4, pp. 995–1006, Feb. 2016.

[40] C. Shi, F. Wang, M. Sellathurai, J. Zhou, and S. Salous, "Power minimization-based robust OFDM radar waveform design for radar and communication systems in coexistence," *IEEE Trans. Signal Process.*, vol. 66, no. 5, pp. 1316–1330, Mar. 2018.

[41] A. Prestel and C. N. Delzell, *Positive Polynomials: From Hilbert's 17th Problem to Real Algebra* (Springer Monographs in Mathematics). Berlin, Germany: Springer, 2001.

[42] B. Dumitrescu, *Positive Trigonometric Polynomials and Signal Processing Applications*. New York, NY, USA: Springer, 2007.

[43] W. Xu, J. Yi, S. Dasgupta, J.-F. Cai, M. Jacob, and M. Cho, "Sepration-free super-resolution from compressed measurements is possible: An orthonormal atomic norm minimization approach," in *Proc. IEEE Int. Symp. Inf. Theory (ISIT)*, Jun. 2018, pp. 76–80.

[44] J.-F. Cai, X. Qu, W. Xu, and G.-B. Ye, "Robust recovery of complex exponential signals from random Gaussian projections via low rank Hankel matrix reconstruction," *Appl. Comput. Harmon. Aanl.*, vol. 41, no. 2, pp. 470–490, Sep. 2016.

[45] A. Panahi and M. Viberg, "Performance analysis of sparsity-based parameter estimation," *IEEE Trans. Signal Process.*, vol. 65, no. 24, pp. 6478–6488, Dec. 2017.
[46] Z. Tan, Y. C. Eldar, and A. Nehorai, "Direction of arrival estimation using co-prime arrays: A super resolution viewpoint," *IEEE Trans. Signal Process.*, vol. 62, no. 21, pp. 5565–5576, Nov. 2014.
[47] D. Goldfarb and K. Scheinberg, "Interior point trajectories in semidefinite programming," *SIAM J. Optim.*, vol. 8, no. 4, pp. 871–886, 1998.
[48] O. Nadiri and B. Rafaely, "Localization of multiple speakers under high reverberation using a spherical microphone array and the direct-path dominance test," *IEEE/ACM Trans. Audio, Speech, Language Process.*, vol. 22, no. 10, pp. 1494–1505, Oct. 2014.
[49] L. Kumar and R. M. Hegde, "Stochastic Cramér-Rao bound analysis for DOA estimation in spherical harmonics domain," *IEEE Signal Process. Lett.*, vol. 22, no. 8, pp. 1030–1034, Aug. 2015.
[50] V. I. Lebedev and A. L. Skorokhodov, "Quadrature formulas of orders 41, 47 and 53 for the sphere," *Russ. Acad. Sci. Dokl. Math.*, vol. 45, no. 3, pp. 587–592, 1992.
[51] L. Madmoni and B. Rafaely, "Direction of arrival estimation for reverberant speech based on enhanced decomposition of the direct sound," *IEEE J. Sel. Topics Signal Process.*, vol. 13, no. 1, pp. 131–142, Mar. 2019.

JIE PAN received the B.Sc. and Ph.D. degrees from the Nanjing University of Aeronautics and Astronautics (NUAA), Nanjing, China, in 2005 and 2013, respectively. He is currently a Lecturer with the School of Information Engineering, Yangzhou University, Yangzhou, China. His current research interests include the direction-of-arrive estimation, array signal processing, and sparse signal representation.